

Overbounding Position Errors in the Presence of Carrier Phase Multipath Error Model Uncertainty

Samer Khanafseh, Steven Langel and Boris Pervan
Illinois Institute of Technology
Chicago, IL

Abstract—In this paper, a methodology is developed to overbound the error in position estimation for carrier phase navigation systems subject to multipath error mis-modeling. In high accuracy and high integrity applications, carrier phase positioning systems with cycle resolution usually rely on time-filtering, in many cases using Kalman filters. Naturally, for a computed integrity risk to be meaningful, it must be guaranteed that the predicted state estimation error covariance always bounds the true covariance. The Kalman filter ensures state error covariance bounding provided that the measurement errors and system dynamics are accurately modeled. However, uncertainties in the dynamic model of the multipath error states always exist. In response, the focus of this work is to quantify and bound position estimate errors subject to uncertainties associated with the time correlation of multipath error.

Keywords—Robust Estimation; Multipath Model; Kalman Filter; Modeling Uncertainty; Overbounding

I. INTRODUCTION

For demanding aviation applications such as autonomous shipboard landing or autonomous airborne refueling, accuracy and integrity of carrier phase positioning and cycle resolution are essential. In such applications, filtering of the carrier phase measurements is usually used to reliably estimate the cycle ambiguities before fixing. In this work, we focus on using the Kalman filter as the fundamental basis for the estimation of the position and ambiguity states. In order to quantitatively evaluate the quality of the cycle ambiguity resolution and the integrity risk in subsequent positioning, the estimate error covariance matrix from the Kalman filter is used.

In navigation, overbounding usually refers to the process of replacing the actual error distribution by a simplified conservative error model. In most applications, a Gaussian distribution is used due to its simplicity and unique characteristics. For example, Gaussian distributions can be defined by only two parameters: the mean and standard deviation, and can be easily propagated through linear filters and estimators such as least squares estimators and Kalman filters. As a result, the estimate error covariance can be applied to the overbounding of the actual estimate errors. For example, the range domain distributions can be related to the position domain and used in computing protection levels or integrity risk. One of the first publications on overbounding the estimate error subject to non-Gaussian measurement distributions for integrity purposes was written by DeCleene [1]. In that work,

he showed that if the CDF of the measurement error is overbounded at every point by a Gaussian CDF, then the covariance of the position estimate using the overbounding Gaussian standard deviation overbounds the actual estimate errors. Extending this work, Rife developed the paired overbounding method for cases where the measurement error CDF is asymmetric, multimodal or non-zero mean [2]. Furthermore, Rife [3] and Pulford [4] worked on overbounding outputs of linear time invariant (LTI) systems driven by random processes which possess a spherically symmetric joint probability density function.

In the context of a Kalman filter, the methods described in [1] and [2] can be applied to overbound the measurement and process noise distributions. That is, if these noise processes can be overbounded using these methods, then it is guaranteed that the estimate error covariance will overbound the actual error covariance. This claim will be true as long as the measurement noise and process noise can be accurately modeled as white noise processes. However, in GPS navigation applications, the measurement noise is often colored due to the presence of multipath. Although the results from [3] and [4] provide the means to handle the time correlated nature of multipath, they are difficult to apply in the context of a Kalman filter, which is typically a time varying system in GPS applications. If this time correlated error is ignored, then the Kalman filter is not optimal anymore because it does not model the actual system. Furthermore, overbounding the estimate error by the estimate covariance is not guaranteed anymore and the computation of protection levels is no longer meaningful. Finally, if cycle ambiguities are to be fixed and the colored nature of the measurement noise is not modeled and accounted for in the Kalman filter, the integrity of cycle resolution will also be at risk [5]. All of these adverse effects caused by ignoring the multipath structure will inevitably jeopardize the integrity risk of the positioning solution.

Provided that the multipath error can be accurately modeled as the output of a linear system driven by white noise, then the method of state augmentation can be used in which the multipath error is modeled as an additional state in the Kalman filter. Unfortunately, an exact statistical description of the colored noise process cannot be precisely known, and hence an approximate model must be considered. For example, in GPS navigation architectures, a first order Gauss Markov process is often used to model multipath. Recognizing that the model itself is only an approximation, and furthermore that the time constant of the model can vary with time and satellite

elevation, it is not immediately clear how the underlying uncertainty due to mis-modeling will affect the bounding characteristics of the resulting positioning solution.

In response, we begin by investigating how uncertainties in the dynamic model affect the nature of the output covariance relative to the true error. These results are then adapted specifically to the mis-modeling of the multipath time constant and its effect on the integrity of the positioning solution. As a basic example in this work, the state vectors considered included different combinations of position, cycle ambiguity, and multipath states. It is assumed that an upper and lower bound can be imposed on the actual multipath time constant. For any true time constant which falls within these limits, it will be shown that no single value of assumed time constant can overbound the actual errors at all epochs. As a result, a minimax optimization problem is proposed here. Recall that the estimation error covariance is ultimately used to verify compliance with navigation integrity risk requirements. However, the ultimate goal is to overbound the position estimation error without excessive conservatism, because aviation applications also typically have stringent availability requirements. The value of the new method is that it satisfies both of these criteria; its solution provides an optimal overbounding covariance that overbounds the actual errors at every instant in time.

In this work, we start by discussing multipath error modeling in navigation systems that use Kalman filters. A simple 1-D example is then defined, which is used as a benchmark for the rest of the analysis in this paper. Using this benchmark example, a Monte-Carlo simulation is conducted and the preliminary results are shown. The sensitivity of the Kalman filter to the dynamic matrix mis-modeling is derived and used to ensure that the output covariance overbounds the actual errors from the Monte-Carlo simulation. Based on these results, the minimax condition is then developed and a preliminary realization of the optimum solution is defined.

II. KALMAN FILTERING WITH MULTIPATH COLORED NOISE

To be general, no assumption is made in this section about the structure of the state vector used in the Kalman filter. In navigation systems, the state vector may include position, cycle ambiguities, or atmospheric states, as an example. Therefore, the measurement equation at time k , which relates the measurements \mathbf{z} to the state vector \mathbf{x} is

$$\mathbf{z}_k = \mathbf{H}_k \mathbf{x}_k + \mathbf{v}_k \quad (1)$$

where \mathbf{H} is the observation matrix.

The dynamic equation that describes the time variation of the state vector is

$$\mathbf{x}_k = \Phi_{k-1} \mathbf{x}_{k-1} + \mathbf{w}_{k-1} \quad (2)$$

where,

Φ_{k-1} : the dynamic transition matrix from epoch $k-1$ to k

\mathbf{w}_{k-1} : the process noise from epoch $k-1$ to k

Based on these equations, the *a priori* estimate $\bar{\mathbf{x}}_k$, its covariance matrix $\bar{\mathbf{P}}_k$, the Kalman gain \mathbf{K}_k , the *a posteriori*

estimate $\hat{\mathbf{x}}_k$, and its covariance matrix $\hat{\mathbf{P}}_k$ can be, respectively, computed as [6],

$$\bar{\mathbf{x}}_k = \Phi_{k-1} \hat{\mathbf{x}}_{k-1} \quad (3)$$

$$\bar{\mathbf{P}}_k = \Phi_{k-1} \hat{\mathbf{P}}_{k-1} \Phi_{k-1}^T + \Gamma_{k-1} \quad (4)$$

$$\mathbf{K}_k = \bar{\mathbf{P}}_k \mathbf{H}_k^T (\mathbf{H}_k \bar{\mathbf{P}}_k \mathbf{H}_k^T + \mathbf{R}_k)^{-1} \quad (5)$$

$$\hat{\mathbf{x}}_k = \bar{\mathbf{x}}_k + \mathbf{K}_k (\mathbf{z}_k - \mathbf{H}_k \bar{\mathbf{x}}_k) \quad (6)$$

$$\hat{\mathbf{P}}_k = (\mathbf{I} - \mathbf{K}_k \mathbf{H}_k) \bar{\mathbf{P}}_k \quad (7)$$

where,

Γ_{k-1} : is the process noise covariance matrix

\mathbf{R}_k : the measurement noise covariance matrix

The derivation of the Kalman filter equations (3-7), assumes that the measurement noise \mathbf{v}_k is white. GPS measurement errors are caused by different sources such as thermal receiver noise, multipath errors and atmospheric associated errors. Although receiver thermal noise can be modeled as white, other error sources such as multipath may have significant time correlation.

In the literature, different techniques exist that facilitate using the Kalman filter with colored measurement noise. One method is to effectively whiten the measurements by re-sampling the measurements at a lower rate such that the new sampled measurements are nearly independent and can be assumed to be white. Although this technique can be successful, it assumes that time intervals needed to ensure independence are known in advance, and its functionality is restrained because the measurement updates are limited to longer periods (several minutes for example). For instance, this approach might not be practical if an Inertial Navigation System (INS) is to be tightly coupled with GPS. In these situations, if measurement updates are to be performed at low rates (sometimes even less than 0.01 Hz), INS errors between successive measurement updates will keep increasing and might cause the system to violate the accuracy and integrity requirements. If measurement updates are performed at higher rates (1Hz, for example) INS sensor biases are corrected faster, thus bounding the INS propagation errors. Another scenario where whitening the measurements is not practical is in cases of severe satellite geometry change due to blockages such as in aircraft banking maneuvers, urban canyon environments, or airborne refueling missions. In these scenarios, satellites might be blocked for short periods of times then reacquired. If the Kalman filter is not capable of bringing these satellites to the navigation solution quickly, the navigation performance will be degraded.

An alternative approach for handling colored measurement noise is by imposing an approximate model for the dynamics of the colored noise. If the dynamics of the colored noise can be adequately modeled using linear system theory, then state augmentation [7] or measurement differencing [8] techniques can be used. Both methods are technically equivalent. The state augmentation approach is more straight forward, but requires additional nuisance states to be added to the filter. In contrast, the measurement differencing filter does not require the addition of these states but is slightly more complex and

computationally demanding. In this work, for simplicity, we will adopt the state augmentation approach. For state augmentation, the measurement noise \mathbf{v}_k is broken into two components: a white noise component, \mathbf{n}_k and a colored noise component, \mathbf{m}_k . The dynamic model for \mathbf{m}_k is assumed to have the following form:

$$\mathbf{m}_k = \mathbf{F}_{k-1} \mathbf{m}_{k-1} + \boldsymbol{\xi}_{k-1} \quad (8)$$

where \mathbf{F} is the dynamic matrix of the colored noise vector, \mathbf{m} , and $\boldsymbol{\xi}_{k-1}$ is the process noise of the augmented state.

Using this model, the augmented states, \mathbf{m} , are appended to the original state vector, \mathbf{x} , transforming the measurement equation (1) and dynamic equation (2) into:

$$\mathbf{z}_k = \begin{bmatrix} \mathbf{H}_k & \mathbf{I} \end{bmatrix} \begin{bmatrix} \mathbf{x} \\ \mathbf{m} \end{bmatrix}_k + \mathbf{n}_k \quad (9)$$

$$\begin{bmatrix} \mathbf{x} \\ \mathbf{m} \end{bmatrix}_k = \begin{bmatrix} \boldsymbol{\Phi}_{k-1} & \mathbf{0} \\ \mathbf{0} & \mathbf{F}_{k-1} \end{bmatrix} \begin{bmatrix} \mathbf{x} \\ \mathbf{m} \end{bmatrix}_{k-1} + \begin{bmatrix} \mathbf{w}_{k-1} \\ \boldsymbol{\xi}_{k-1} \end{bmatrix} \quad (10)$$

GPS multipath error is usually modeled as a first order Gauss-Markov process [5]. For simplicity, if we assume that all multipath states for all satellites have the same time constant τ and using the discrete form of the first order Gauss-Markov process, the \mathbf{F} matrix in (10) becomes,

$$\mathbf{F}_{k-1} = \exp(-\Delta t / \tau) \mathbf{I} \quad (11)$$

where Δt is the sampling period. If the same standard deviation of the driving noise σ_ξ^2 is also used for all multipath states, the process noise covariance matrix of $\boldsymbol{\xi}_{k-1}$ becomes,

$$\mathbf{Q}_{k-1} = \sigma_\xi^2 (1 - \exp(-2\Delta t / \tau)) \mathbf{I} \quad (12)$$

In this work we acknowledge that using the first order Gauss-Markov model to model multipath might not represent the actual multipath error exactly but we will assume that it is an adequate approximation. However, what value to use for the time constant is an open question. In certain applications where the antennas are installed in a fixed environment, collected data can be post processed to estimate the time constant. Nevertheless, this process is not trivial. In order to get a representative estimate on the time constant, the thermal noise must be first separated from the multipath measurement noise. If a low pass filter is used for this purpose, the time constant of this low pass filter must be chosen carefully. For instance, the low pass filter time constant should be large enough to average out the thermal noise, thus leaving only the multipath, but not too large to interfere with the multipath time constant estimation. With the actual time constant being unknown, an iterative process of changing the low pass filter might be necessary until a convergence on the time constant is achieved. Also, in order to have a reliable estimate on the time constant, many data samples are needed, which is not always achievable for every satellite (due to short passes). Finally, even if multipath could be separated and enough data points exist, the multipath time constant may not be time invariant. Multipath error is a function of the environment and the

satellite geometry with respect to the surroundings, which implies that the time constant is also a function of the environment and satellite geometry. In conclusion, although a rough estimate of the multipath time constant can be obtained by post processing data, an accurate estimate can never be achieved. This uncertainty in the estimate impacts the optimality of the Kalman filter. As a result errors will be induced in the state estimate and the covariance might not be conservative, which in turn does not guarantee that the computed position estimate error is overbounding the actual error.

Perhaps an accurate estimate of the multipath time constant is unreachable, but a bound on the time constant estimate can be assumed. Using these bounds, the goal is to provide a covariance that always overbounds the actual estimate errors. The broad literature on robust estimation provides two different solutions to such a problem: the *Robust Kalman Filter (RKF)* [9] and the H_∞ filter [10]. However, these filters present some practical difficulties that may make them unsuitable for navigation systems in aviation applications. For example, both filters need to be checked for stability at every epoch. In order to keep the filters stable, certain design and tuning parameters must be changed on-the-fly. These parameters can cause the covariance to be overly conservative for aviation navigation systems with high availability requirements. Furthermore, it is quite challenging to quantify the integrity risk of these systems as a function of the tuning parameters. In response, we pursue an alternative approach to this problem where we provide a covariance that overbounds the true error for an actual time constant that is bounded by τ_1 and τ_2 ($\tau \in [\tau_1, \tau_2]$). However, before we pursue the alternative approach, let us examine the impact of mis-modeling the time constant on a simple 1-D estimation example using a Kalman filter estimator (3-7) in a Monte-Carlo simulation.

III. MONTE-CARLO SIMULATION

For simplicity, we will use a 1-D estimation example that estimates one position and one ambiguity state. In generating the measurements, we assume that the ambiguity value is constant and equal to 7 and that the position is static and fixed with a value of 1. Thermal noise n_k is generated using zero mean and a standard deviation of 0.5 cm (mimicking a carrier phase thermal noise). Multipath m_k is generated using a first order Gauss Markov model with a fixed time constant of 100 seconds and a standard deviation on the process noise of 1.0 cm. The measurement noise is then formed by adding the thermal noise to the colored multipath error at 1Hz. The measurement noise is then added to the actual measurement consisting of the range and ambiguity as shown in (13), the measurement equation at time epoch k .

$$z_k = k \times 1 + 7 + m_k + n_k \quad (13)$$

where the scalar multiplier k represents the geometry change in time. A sample of the resultant measurement is shown in Figure 1.

In the estimation process, the 1-D measurement and dynamic model equations including the multipath state are written as,

$$z_k = \begin{bmatrix} k & 1 & 1 \end{bmatrix} \begin{bmatrix} x \\ a \\ m \end{bmatrix}_k + n_k \quad (14)$$

$$\begin{bmatrix} x \\ a \\ m \end{bmatrix}_k = \begin{bmatrix} 1 & 0 & 0 \\ 0 & 1 & 0 \\ 0 & 0 & \exp(-1/\tau_e) \end{bmatrix} \begin{bmatrix} x \\ a \\ m \end{bmatrix}_{k-1} + \begin{bmatrix} 0 \\ 0 \\ \xi_{k-1} \end{bmatrix} \quad (15)$$

where x is the position state, a is the ambiguity state, and τ_e is the time constant that is used in the estimation process and might be different than τ .

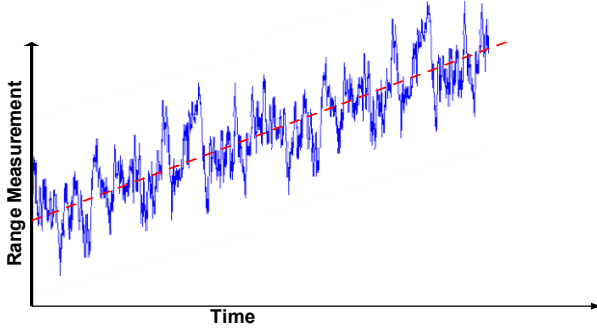


Figure 1. Sample of the simulated measurement of the example in (13).

The state estimates are initialized with zeros and the initial covariance is initialized with a diagonal matrix where the elements corresponding to the position and ambiguity states are initialized with 1×10^6 (to show the lack of information about the accuracy of the initial guess). The initial covariance for the multipath state is initialized with the value σ_ξ^2 (which is 1×10^{-4}).

This Monte Carlo simulation is performed using 10,000 runs with 1000 epochs per run. In the estimation process, we will assume that we do not know the actual time constant but have bounds on it as ($20 < \tau < 400$). As a first attempt, let us assume that we will use $\tau_e = 20$ sec in the estimator. Figure 2 shows the position estimate error for 10 runs of the Monte-Carlo simulation (in blue) with the predictive standard deviation on the position estimate error (in red) obtained from the Kalman filter covariance matrix.

Since it is not easy to judge if the predictive covariance (1σ) represents the actual error standard deviation, the sample variance of the actual estimate error over all 10,000 runs is computed and compared to the predictive variance. Because the sample size is still limited, a $\pm 1\sigma$ error band on the estimation of the sample position estimate error variance is also shown in Figure 3 (due to the scale of the position error, the bands collapse to form a thick line). In the rest of the paper, this representation will be used to compare the actual estimate error to the predictive covariance. It is clear now that the predictive variance overbounds the actual error for the first 150 epochs. Afterwards, the predictive variance becomes overly optimistic compared to the actual error. This case shows that if protection levels in a certain navigation application are computed using this predictive variance, (computed using a time constant of 20 seconds) these protection levels will not overbound at all times the actual errors with a sufficient

probability that meets the integrity risk requirements. As a result, the integrity of the estimate is at risk.

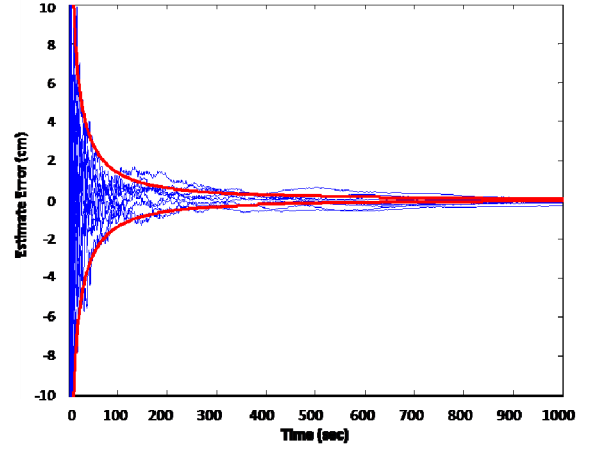


Figure 2. Position state estimates for different Monte-Carlo runs (blue) and the predictive standard deviation (red) when the estimator uses 20 seconds as a multipath time constant.

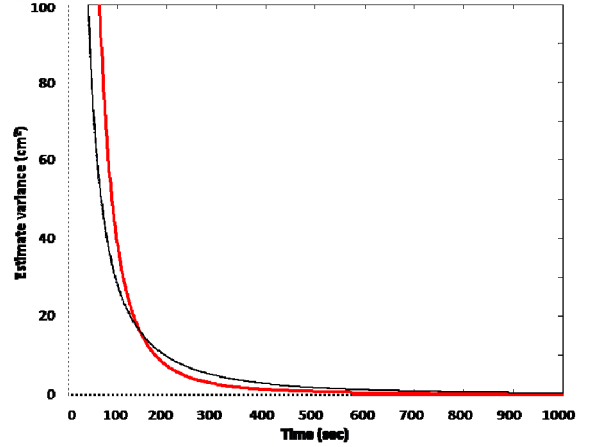


Figure 3. The sample variance of the actual position estimate error (black) and the predictive variance (red) for the case in Figure 2.

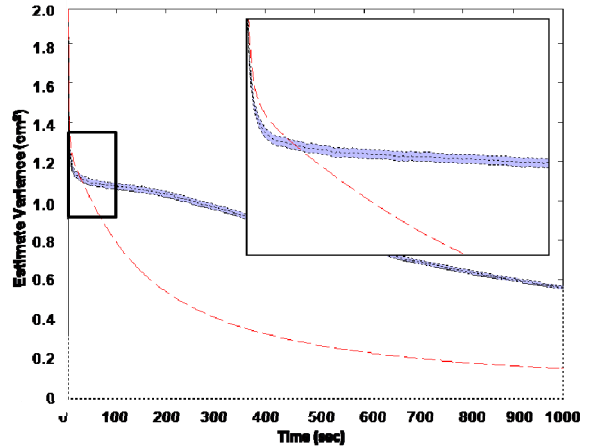


Figure 4. The sample variance of the actual ambiguity estimate error (black) and the predictive variance (red) for the case in Figure 2.

If the same process is applied to the cycle ambiguity estimate (Figure 4), the same observation can also be made. The variance of the estimate error is overly optimistic after 60 epochs. If this covariance matrix is used afterwards for cycle resolution, the computed probability of correctly fixing the ambiguities will be meaningless and the integrity of the final position solution will be as well.

Similar plots are made for the case where the other bound of τ_e is used (400 sec) and these results are shown in Figure 5. Using the upper bound of the time constant in the estimator it is clear that the predictive variance overbounds the actual errors for epochs beyond 820 seconds for position and 170 seconds for the ambiguity estimate. But for epochs before 820 epochs, the covariance is overly optimistic. Therefore, it will also cause a breach in the computed integrity risk. On the other hand, if the actual time constant (100 sec) is used as τ_e , the variance of the estimate matches the actual estimate error (Figure 6). In conclusion, this simple numerical experiment shows that, there is no single value for the multipath time constant that results in a predictive covariance matrix that overbounds the actual errors at all epochs. The only exception is using the actual time constant. However, in reality, the

actual time constant is unknown and might be changing with time.

Since the goal is to provide a predictive covariance that always overbounds the actual errors at all epochs for all time constant values ($20 < \tau_e < 400$), one might think that evaluating the maximum of the position variance (or alternatively, the trace of the covariance matrix) guarantees that the actual errors are always overbounded and be conservative. However, the definition of the covariance in this case is not representative of how the estimator is behaving. Specifically, in the derivation of the estimate error covariance of the Kalman filter, it is assumed that the dynamic model of the actual system is the same as the dynamic model of the estimator. If the estimator time constant τ_e is to be changed based on the maximization condition mentioned earlier, the predictive covariance is assuming that the actual time constant is changing in the same manner, which might not be the case. Therefore, we need to define the covariance of the estimate error given that the estimator and the actual system have different dynamic matrices (Φ) before trying to optimize and find the most conservative covariance.

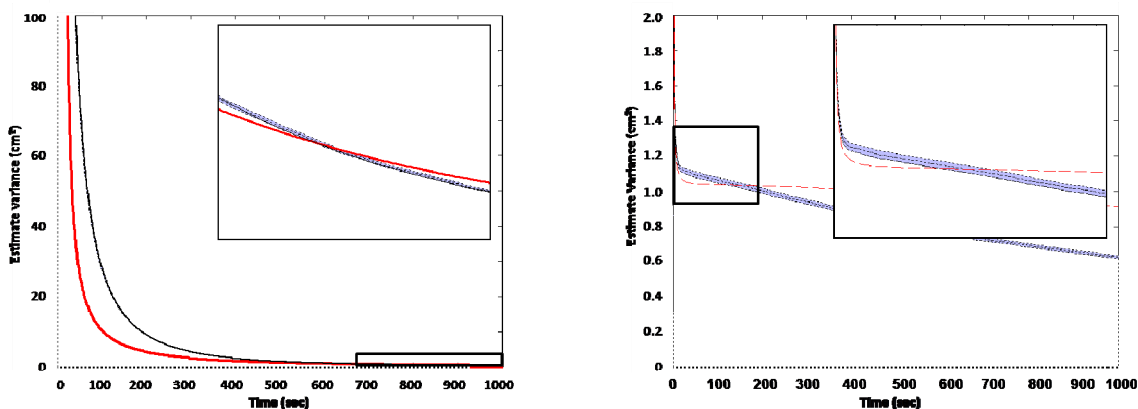


Figure 5. The sample variance of the actual estimate error (black) and the predictive variance (red) for the position (left) and ambiguity (right) states when the estimator uses 400 seconds as a multipath time constant.

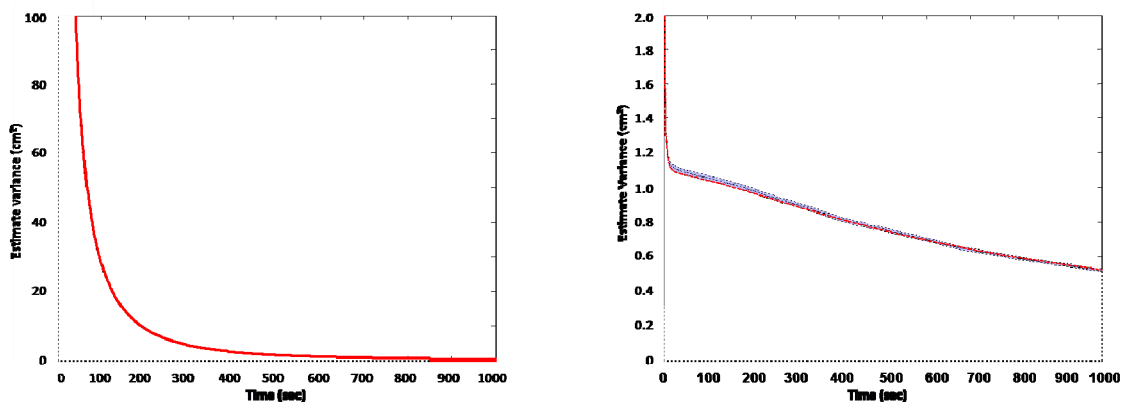


Figure 6. The sample variance of the actual estimate error (black) and the predictive variance (red) for the position (left) and ambiguity (right) states when the estimator uses 100 seconds as a multipath time constant

IV. MODIFIED ESTIMATE ERROR COVARIANCE

In this section, we will show the derivation of the estimate error covariance given that the actual system dynamic matrix is different from the dynamic matrix of the estimator ($\tilde{\Phi}$). This derivation can be found in several estimation text books under section titles such as ‘‘sensitivity of the Kalman filter’’ or ‘‘error analysis’’ [6,7,11].

As shown in Equation 2, let us assume that the actual system dynamic equation is

$$\mathbf{x}_k = \Phi_{k-1} \mathbf{x}_{k-1} + \mathbf{w}_{k-1} \quad (16)$$

while the *a priori* estimator is based on different dynamic matrix ($\tilde{\Phi}$) as,

$$\bar{\mathbf{x}}_k = \tilde{\Phi}_{k-1} \hat{\mathbf{x}}_{k-1} \quad (17)$$

Then the *a priori* estimate error $\bar{\mathbf{e}}$, which is defined as $\bar{\mathbf{e}}_k = \bar{\mathbf{x}}_k - \mathbf{x}_k$, is given by:

$$\bar{\mathbf{e}}_k = \bar{\mathbf{x}}_k - \mathbf{x}_k = \tilde{\Phi}_{k-1} \hat{\mathbf{x}}_{k-1} - \Phi_{k-1} \mathbf{x}_{k-1} - \mathbf{w}_{k-1} \quad (18)$$

It can be seen that unlike the regular Kalman filter, the term $\hat{\mathbf{x}}_k - \mathbf{x}_k$ (which can be referred to as $\hat{\mathbf{e}}_k$) cannot be explicitly obtained. The vector $\hat{\mathbf{e}}_k$ is the *a posteriori* estimate error, which can be derived from the measurement update step. By adding and subtracting the term $\tilde{\Phi}_{k-1} \mathbf{x}_{k-1}$ from (18):

$$\begin{aligned} \bar{\mathbf{e}}_k &= \tilde{\Phi}_{k-1} (\hat{\mathbf{x}}_{k-1} - \mathbf{x}_{k-1}) + (\tilde{\Phi}_{k-1} - \Phi_{k-1}) \mathbf{x}_{k-1} - \mathbf{w}_{k-1} \\ &= \tilde{\Phi}_{k-1} \hat{\mathbf{e}}_{k-1} + \Delta\Phi_{k-1} \mathbf{x}_{k-1} - \mathbf{w}_{k-1} \end{aligned} \quad (19)$$

where $\Delta\Phi = \tilde{\Phi} - \Phi$. We can rewrite (19) in matrix form by augmenting the state vector \mathbf{x} to the error vector \mathbf{e} as,

$$\begin{bmatrix} \bar{\mathbf{e}}_k \\ \mathbf{x}_k \end{bmatrix} = \begin{bmatrix} \tilde{\Phi}_{k-1} & \Delta\Phi_{k-1} \\ \mathbf{0} & \Phi_{k-1} \end{bmatrix} \begin{bmatrix} \hat{\mathbf{e}}_{k-1} \\ \mathbf{x}_{k-1} \end{bmatrix} + \begin{bmatrix} -\mathbf{I} \\ \mathbf{I} \end{bmatrix} \mathbf{w}_{k-1} \quad (20)$$

The error term $\bar{\mathbf{e}}_k$ in (20) represents the actual estimate error when different dynamics is present in the estimator and the actual system, and the resulting actual estimator error covariance is

$$\begin{aligned} E \left\{ \begin{bmatrix} \bar{\mathbf{e}}_k \\ \mathbf{x}_k \end{bmatrix} \begin{bmatrix} \bar{\mathbf{e}}_k \\ \mathbf{x}_k \end{bmatrix}^T \right\} &= \\ & \begin{bmatrix} \tilde{\Phi}_{k-1} & \Delta\Phi_{k-1} \\ \mathbf{0} & \Phi_{k-1} \end{bmatrix} \begin{bmatrix} \hat{\mathbf{e}}_{k-1} \\ \mathbf{x}_{k-1} \end{bmatrix} \begin{bmatrix} \tilde{\Phi}_{k-1} & \Delta\Phi_{k-1} \\ \mathbf{0} & \Phi_{k-1} \end{bmatrix}^T \\ & + \begin{bmatrix} \mathbf{Q}_{k-1} & -\mathbf{Q}_{k-1} \\ -\mathbf{Q}_{k-1} & \mathbf{Q}_{k-1} \end{bmatrix} \end{aligned} \quad (21)$$

The measurement update step is more direct, and the *a posteriori* error can be shown to be

$$\hat{\mathbf{e}}_k = (\mathbf{I} - \mathbf{K}_k \mathbf{H}_k) \bar{\mathbf{e}}_k + \mathbf{K}_k \mathbf{v}_k \quad (22)$$

where \mathbf{K} is the Kalman gain using the assumed estimator model $\tilde{\Phi}$. Thus, to be consistent with the augmented system in (20), the measurement update equation becomes

$$\begin{bmatrix} \hat{\mathbf{e}}_k \\ \mathbf{x}_k \end{bmatrix} = \begin{bmatrix} (\mathbf{I} - \mathbf{K}_k \mathbf{H}_k) & \mathbf{0} \\ \mathbf{0} & \mathbf{I} \end{bmatrix} \begin{bmatrix} \bar{\mathbf{e}}_k \\ \mathbf{x}_k \end{bmatrix} + \begin{bmatrix} \mathbf{K}_k \\ \mathbf{0} \end{bmatrix} \mathbf{v}_k, \quad (23)$$

and its covariance is

$$\begin{aligned} E \left\{ \begin{bmatrix} \hat{\mathbf{e}}_k \\ \mathbf{x}_k \end{bmatrix} \begin{bmatrix} \hat{\mathbf{e}}_k \\ \mathbf{x}_k \end{bmatrix}^T \right\} &= \\ & \begin{bmatrix} (\mathbf{I} - \mathbf{K}_k \mathbf{H}_k) & \mathbf{0} \\ \mathbf{0} & \mathbf{I} \end{bmatrix} \begin{bmatrix} \bar{\mathbf{e}}_k \\ \mathbf{x}_k \end{bmatrix} \begin{bmatrix} (\mathbf{I} - \mathbf{K}_k \mathbf{H}_k) & \mathbf{0} \\ \mathbf{0} & \mathbf{I} \end{bmatrix}^T \\ & + \begin{bmatrix} \mathbf{K}_k \mathbf{R}_k & \mathbf{0} \\ \mathbf{0} & \mathbf{0} \end{bmatrix} \end{aligned} \quad (24)$$

Equations (21) and (24) are used to propagate the modified covariance along with the Kalman filter time and measurement updates of the state vector. At each epoch, the upper left 3×3 block matrix (corresponding to the covariance of $\hat{\mathbf{e}}_k$) is then extracted as the modified predictive covariance of the estimate error ($\tilde{\mathbf{P}}$).

The initialization of the modified covariance estimation is carried out as follows:

$$E \left\{ \begin{bmatrix} \hat{\mathbf{e}}_0 \\ \mathbf{x}_0 \end{bmatrix} \begin{bmatrix} \hat{\mathbf{e}}_0 \\ \mathbf{x}_0 \end{bmatrix}^T \right\} = \begin{bmatrix} E\{\hat{\mathbf{e}}_0 \hat{\mathbf{e}}_0^T\} & E\{\hat{\mathbf{e}}_0 \mathbf{x}_0^T\} \\ E\{\mathbf{x}_0 \hat{\mathbf{e}}_0^T\} & E\{\mathbf{x}_0 \mathbf{x}_0^T\} \end{bmatrix} \quad (25)$$

Since \mathbf{x}_0 is a random variable that can be expressed as $\hat{\mathbf{x}}_0 - \hat{\mathbf{e}}_0$, the term $E\{\mathbf{x}_0 \mathbf{x}_0^T\}$ can be written in terms of an initial guess on the state vector $\hat{\mathbf{x}}_0$ (which is a deterministic vector) and $\hat{\mathbf{e}}_0$ which is a random vector error on the guess:

$$\begin{aligned} E\{\mathbf{x}_0 \mathbf{x}_0^T\} &= E\{(\hat{\mathbf{x}}_0 - \hat{\mathbf{e}}_0)(\hat{\mathbf{x}}_0 - \hat{\mathbf{e}}_0)^T\} \\ &= \hat{\mathbf{x}}_0 \hat{\mathbf{x}}_0^T + E\{\hat{\mathbf{e}}_0 \hat{\mathbf{e}}_0^T\} \end{aligned} \quad (26)$$

Applying a similar approach for the off diagonal term $E\{\hat{\mathbf{e}}_0 \mathbf{x}_0^T\}$ results in,

$$E\{\hat{\mathbf{e}}_0 \mathbf{x}_0^T\} = E\{\hat{\mathbf{e}}_0 (\hat{\mathbf{x}}_0 - \hat{\mathbf{e}}_0)^T\} = -E\{\hat{\mathbf{e}}_0 \hat{\mathbf{e}}_0^T\} \quad (27)$$

Substituting (26) and (27) into (25), and defining $\mathbf{P}_0 = E\{\hat{\mathbf{e}}_0 \hat{\mathbf{e}}_0^T\}$ we obtain,

$$E \left\{ \begin{bmatrix} \hat{\mathbf{e}}_0 \\ \mathbf{x}_0 \end{bmatrix} \begin{bmatrix} \hat{\mathbf{e}}_0 \\ \mathbf{x}_0 \end{bmatrix}^T \right\} = \begin{bmatrix} \hat{\mathbf{P}}_0 & -\hat{\mathbf{P}}_0 \\ -\hat{\mathbf{P}}_0 & \hat{\mathbf{P}}_0 + \hat{\mathbf{x}}_0 \hat{\mathbf{x}}_0^T \end{bmatrix} \quad (28)$$

In order to validate $\tilde{\mathbf{P}}$, the same Monte-Carlo simulation is conducted but with the additional computation of (21) and (24), which are initialized with (28), to be the modified predictive covariance. Notice that for the 1D example that is considered in this work, the states are initialized with zero values and therefore the term $\hat{\mathbf{x}}_0 \hat{\mathbf{x}}_0^T$ can be eliminated from (28). Notice that in this computation, both $\tilde{\Phi}$ (requiring the actual time constant of 100 seconds) and $\tilde{\mathbf{\Theta}}$ (including the time constant that is used in the estimator τ_e) are necessary. For this validation step, we will assume that we have access to the actual time constant, but will try different values for τ_e . Figure 7 and 8 show that the $\tilde{\mathbf{P}}$ matches the variance of the actual estimate error for both boundaries of τ_e (20 and 400 seconds).

Therefore, as long as the actual time constant is known, $\tilde{\mathbf{P}}$ will always provide a predictive covariance that matches the actual error variance regardless of τ_e .

These results validate that the methodology to generate the modified predictive covariance is fundamentally correct. In reality, however, the actual time constant is unknown and the only information given is that it is bounded by a certain range of time constant (in our example, 20 and 400 seconds). Therefore, as an experiment, let us fix the estimator time constant (τ_e) to 50 seconds and vary the time constant that the $\tilde{\mathbf{P}}$ equation “thinks” is the actual time constant (τ'_e) in the bounding range 20 to 400 seconds.

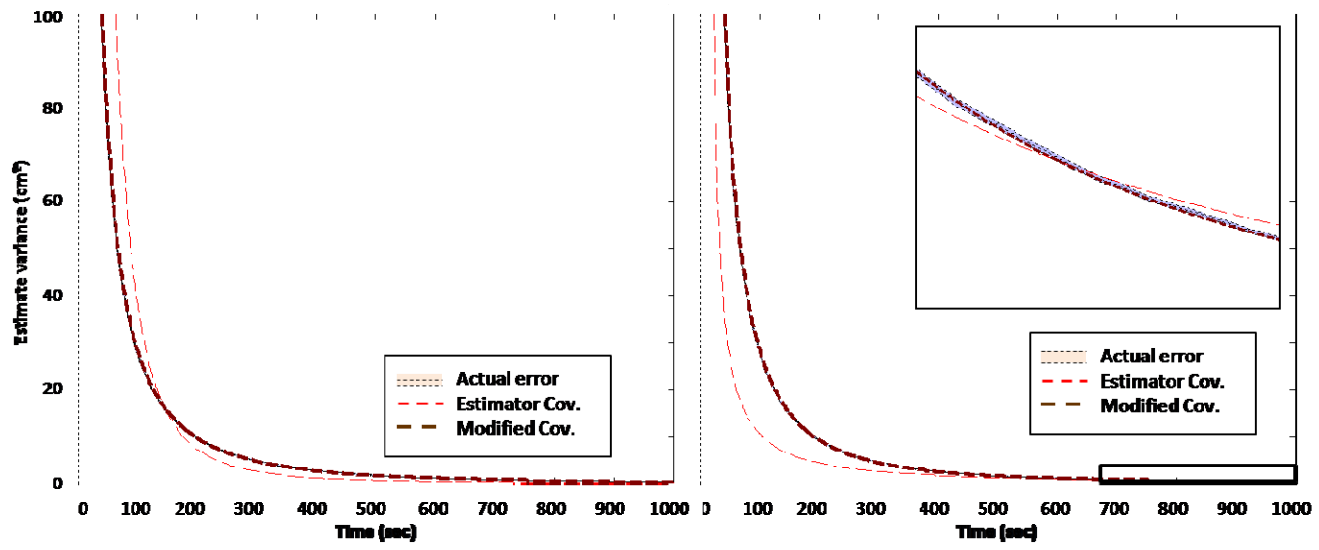


Figure 7. The sample variance of the actual estimate error (black), the predictive variance (red), and the modified variance (dashed brown) for the position (left) and ambiguity (right) states when the estimator uses 20 seconds as time constant

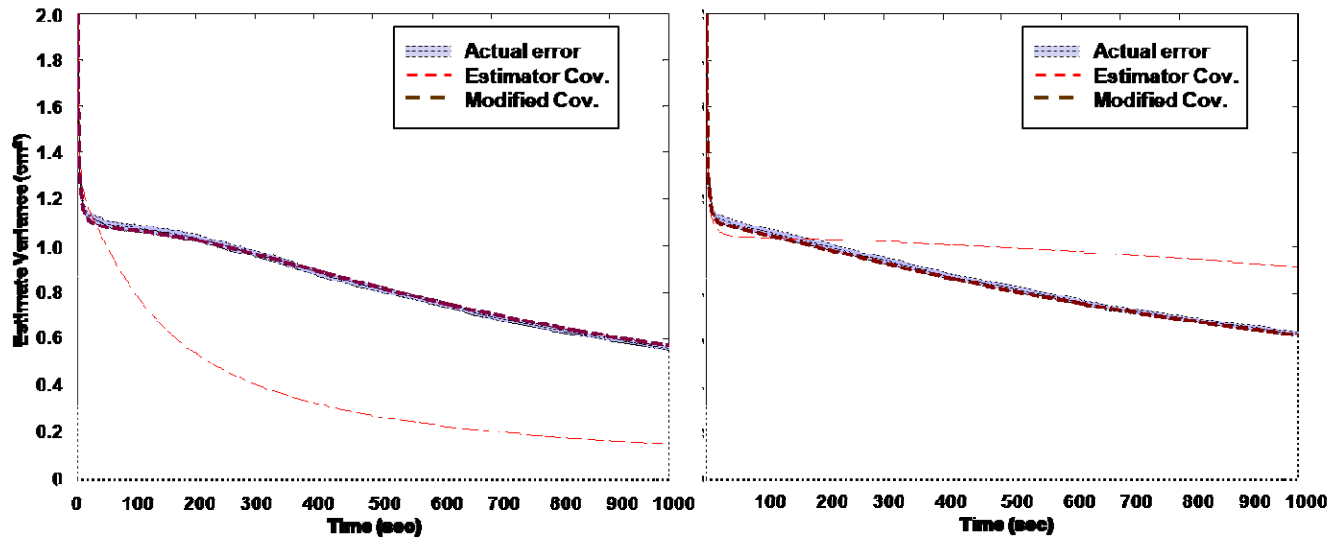


Figure 8. The sample variance of the actual estimate error (black), the predictive variance (red), and the modified variance (dashed brown) for the position (left) and ambiguity (right) states when the estimator uses 400 seconds as time constant

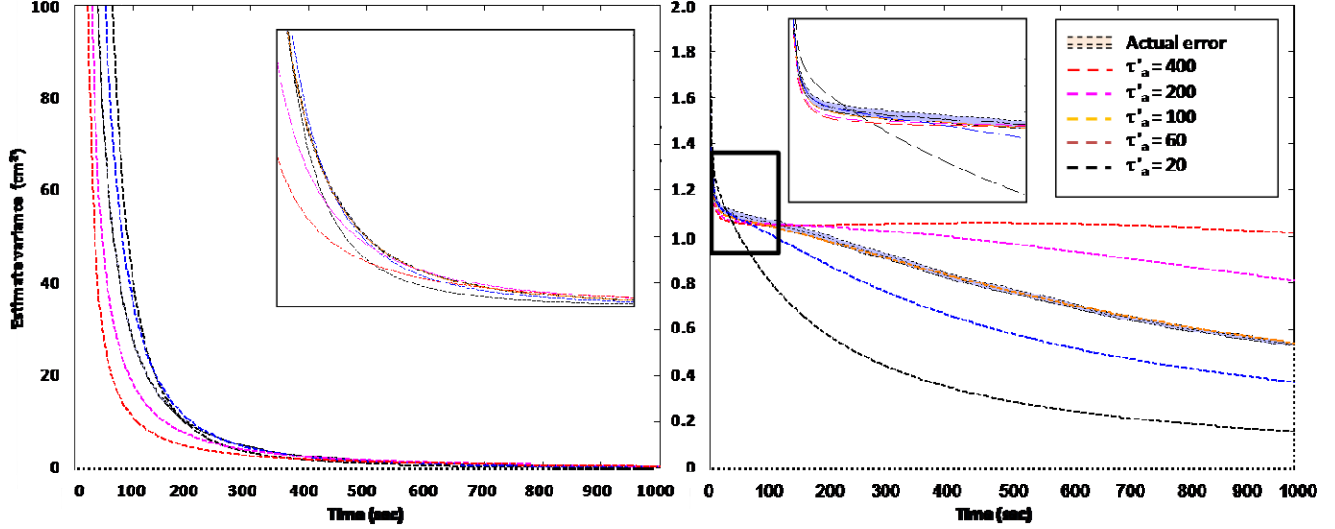


Figure 9. The sample variance of the actual estimate error (black), and the modified variance for the position (left) and ambiguity (right) states for different values of τ'_a

Figure 9 shows the results where each predictive covariance curve corresponds to a value of τ'_a that is used. Although no single value of τ'_a guarantees that the predictive covariance overbounds the actual error all the time, at any instant, the maximum predictive covariance overbounds or matches the actual error. Therefore, for an arbitrary value of τ_e , if the predictive covariance $\tilde{\mathbf{P}}$ is maximized over all values of τ'_a in the range 20 to 400 seconds, the actual errors will always be overbounded. Building on this idea, we will try to define an optimization problem and solve it for the overbounding predictive covariance.

V. MINIMAX OPTIMIZATION

In the previous section we concluded that, for any arbitrary τ_e , the overbounding covariance is the maximum of $\tilde{\mathbf{P}}$ over all values of τ'_a in the bounding range. This maximization can be based on either one element in $\tilde{\mathbf{P}}$ (the position state, for example), the trace of a sub matrix of $\tilde{\mathbf{P}}$ (position and ambiguity) or just the full trace of $\tilde{\mathbf{P}}$. This is left optional for the designer and subject to the integrity requirements of the problem at hand. For example, in our benchmark example, we are not interested in overbounding the multipath state error. Instead, due to its direct impact on integrity, we desire to overbound the ambiguity and position estimates. So, the trace of the upper left 2×2 block of $\tilde{\mathbf{P}}$ is used.

Notice that so far, $\tilde{\mathbf{P}}$ is computed using an arbitrary value of τ_e , but $\tilde{\mathbf{P}}$ overbounds the actual error regardless of the value of τ_e . In order to limit the conservatism and minimize the covariance, the trace of $\tilde{\mathbf{P}}$ can then be minimized for all values of τ_e in the bounding range. In other words, we want to maximize the trace (or selected elements) of $\tilde{\mathbf{P}}$ for all values of τ'_a but minimize this maximum value for all values of τ_e .

Therefore, the optimized overbounding covariance can be written in a mathematical form as,

$$\begin{cases} \tau'_a = \arg \min_{\tau'_a} \left\{ \text{tr} \left[\tilde{\mathbf{P}}(\tau'_a, \tau_e) \right] \right\} \\ \tau'_e = \arg \min_{\tau'_e} \left\{ \text{tr} \left[\tilde{\mathbf{P}}(\tau'_a, \tau'_e) \right] \right\} \end{cases} \quad \forall (\tau'_a, \tau'_e) \in [\tau_1, \tau_2] \quad (29)$$

$$\mathbf{P}^* = \tilde{\mathbf{P}}(\tau'_a, \tau'_e)$$

Unfortunately, solving (29) analytically is quite challenging even for the simple example at hand. At present, an elegant and computationally efficient numerical solution to (29) is not available. Issues such as the convexity of the cost function, Kalman filter memory, and modified covariance memory from previous sub-optimal epochs have not yet been addressed. In response, the only assured way to optimize and solve (29) is by brute force and running a “matrix” of Kalman filters for all values of τ'_a and τ_e in the range 20 to 400 seconds.

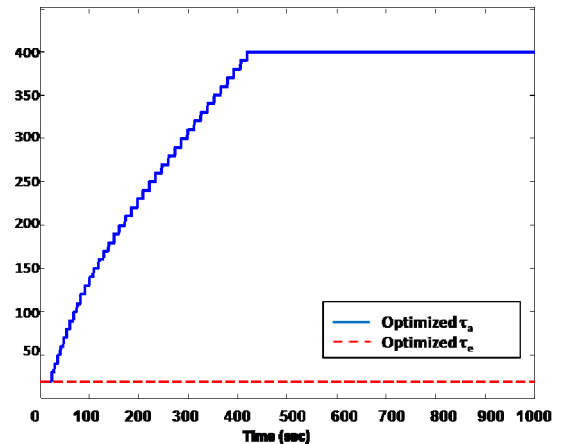


Figure 10. Optimized τ'_a and τ_e .

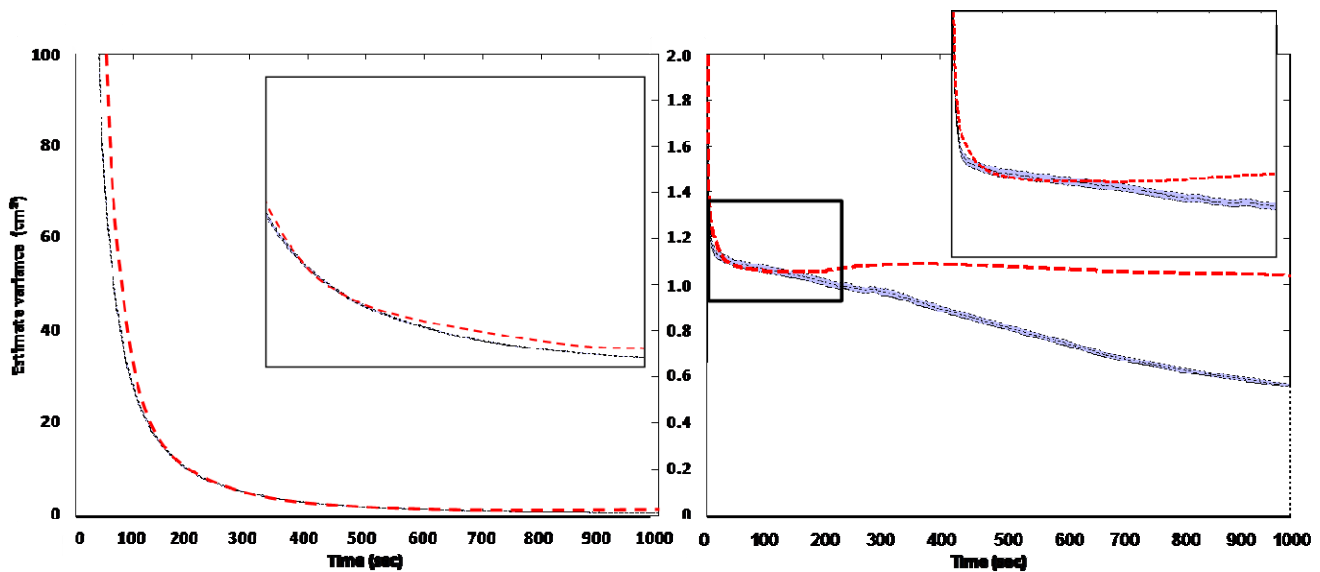


Figure 11. The sample variance of the actual estimate error (black), and the optimized overbounding variances for the position (left) and ambiguity (right) states

By running the matrix of Kalman filters and choosing \mathbf{P}^* subject to (29) for the example in consideration, τ'_a and τ_e that optimize the solution are shown in Figure 10. It can be seen that τ'_a (blue curve) starts with small values and increases with time, which is what was expected by looking at Figure 9. Small τ'_a values lead to overbound of the actual errors for the first few epochs, but as the time goes by larger values of τ'_a are required. The variation in τ_e curve (red dashed curve), on the other hand, is trying to minimize the trace of the position and ambiguity state covariance. The overbounding variances are compared to the actual errors for these values of τ'_a and τ_e in Figure 11. As expected, the optimized minimax variances always overbound, or at least match, the actual estimate errors for all epochs.

VI. SUMMARY AND FUTURE WORK

In this work, we investigated how uncertainties in the dynamic model of the Kalman filter affect the nature of the output covariance relative to the true estimate error. Specifically, we looked at mis-modeling the multipath time constant and its effect on the integrity of an example positioning solution. In that respect, it was concluded that in general, no single value of assumed time constant can overbound the actual errors at all epochs. In response, a modified covariance computation is necessary to take into account multipath mis-modeling. Using the modified covariance, a minimax optimization problem was defined. The optimized minimax covariance is based on maximizing the modified covariance for all values of the actual time constant in a bounding range and minimizing it for all potential values of estimator time constant in the same range. A matrix of Kalman filters was implemented to solve for the optimized covariance.

For future work, we will look into analytically optimizing of the minimax problem, or alternatively to provide a more efficient numerical solution. In the long run, we would be interested in applying the developed techniques to full

navigation systems with different states. For example, INS systems usually model accelerometer and gyro biases as first order Gauss Markov processes with a fixed time constant. Optimizing these systems for a range of time constant will help ensure the system integrity. Furthermore, carrying this research beyond the first order Gauss Markov model to higher orders or even using other models for multipath will also be investigated.

ACKNOWLEDGMENT

The authors gratefully acknowledge the Naval Air Systems Command (NAVAIR) of the US Navy for supporting this research. The authors would like to specifically acknowledge the support and guidance of Glenn Colby and Marie Lage regarding this work. However, the opinions discussed here are those of the authors and do not necessarily represent those of the U.S. Navy or any other affiliated agencies.

REFERENCES

- [1] B. DeCleene, "Defining Pseudorange Integrity - Overbounding," *Proceedings of the 13th International Technical Meeting of the Satellite Division of The Institute of Navigation (ION GPS 2000)*, Salt Lake City, UT, September 2000, pp. 1916-1924.
- [2] J. Rife, S. Pullen, P. Enge, and B. Pervan, "Paired Overbounding for Nonideal LAAS and WAAS Error Distributions," *IEEE Transactions on Aerospace and Electronic Systems*, Vol. 42, No. 4, October 2006, pp. 1386-1395.
- [3] J. Rife, D. Gebre-Egziabher, "Symmetric Overbounding of Correlated Errors," *NAVIGATION*, Vol. 54, No. 2, Summer 2007, pp. 109-124.
- [4] G. Pulford, "A Proof of the Spherically Symmetric Overbounding Theorem For Linear Systems," *NAVIGATION*, Vol. 55, No. 4, Winter 2008-2009, pp. 283-292.
- [5] K. O'Keefe, M. Petovello, G. Lachapelle, E. Cannon, "Assessing Probability of Correct Ambiguity Resolution in the Presence of Time-Correlated Errors," *NAVIGATION*, Vol. 53, No. 4, Winter 2006-2007, pp. 269-282.
- [6] A. Gelb, *Applied Optimal Estimation*. The MIT Press, Cambridge, MA, 1974.
- [7] J. Crassidis and J. Junkins, *Optimal Estimation of Dynamic Systems*. New York, NY: Capman & Hall/CRC, 2004.

- [8] A. Bryson, *Applied Linear Optimal Control: Examples and Algorithms*. New York, NY: Cambridge University Press 2002.
- [9] F. Lewis, L. Xie, D. Popa, *Optimal and Robust Estimation: With an Introduction to Stochastic Control Theory, Second Edition*. CRC Press, 2007.
- [10] D. Simon, *Optimal State Estimation: Kalman, H_∞ and Nonlinear Approaches*. John Wiley and Sons, Hoboken, NJ, 2006.
- [11] Y. Bar-Shalom, X. Li, T. Kirubarajan, *Estimation with Applications to Tracking and Navigation*. New York, NY, 2001.